Jurnal Teknologi

Full paper

Thermal Hydrogen Reduction for Synthesis of Gold Nanoparticles in the Nanochannels of Mesoporous Silica Composite

Mohamad Azani Jalani[a], Leny Yuliati[b], Hendrik O. Lintang[b*]

[a]*Department of Chemistry, Faculty of Science, Universiti Teknologi Malaysia, 81310 UTM Johor Bahru, Johor, Malaysia*
[b]*Ibnu Sina Institute for Fundamental Science Studies, Universiti Teknologi Malaysia, 81310 UTM Johor Bahru, Johor, Malaysia*

*Corresponding author: hendrik@ibnusina.utm.my

Article history

Received :13 October 2013
Received in revised form :
28 January 2014
Accepted :4 February 2014

Graphical abstract

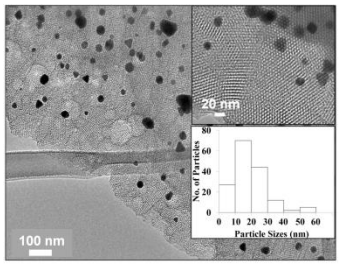

Abstract

Gold nanoparticles (**AuNPs)** with small particle size have been difficult to be synthesized due to their strong agglomeration. Herein we report that the nanochannels of mesoporous silica synthesized from template sol-gel synthesis were utilized to prepare **AuNPs** by employing thermal hydrogen reduction. Mesoporous silica composite with an interpore distance of 4.1 nm was successfully fabricated as a thin film by an amphiphilic trinuclear gold(I) pyrazolate complex (**[Au3Pz3]C10TEG)** as a template. In contrast to calcination method of this composite and the bulk **[Au3Pz3]C10TEG** complex at 450ºC for 3 h, thermal hydrogen reduction at 250ºC for 2 h showed transmission electron microscope (TEM) images and diffraction pattern with smaller particle size (14.5 nm) and more homogenous distribution of **AuNPs** with up to 44% of the particle size in the range of 10 to 20 nm. The decreasing of average particle size in this new strategy indicated by the red-shifting of the surface plasmon resonance (SPR) band from 518 (**AuNPs** from the bulk **[Au3Pz3]C10TEG** complex) and 544 (calcination) to 558 nm.

Keywords: Gold nanoparticles; mesoporous silica composite; particle size; thermal hydrogen reduction

Abstrak

Emas berzarah nano (**AuNPs**) dengan saiz yang kecil adalah amat sukar untuk disintesis disebabkan penggumpalan. Justeru, kajian ini melaporkan nanokomposit lapisan silika yang disintesis melalui proses sol-gel boleh digunapakai untuk menyediakan **AuNPs** menggunakan penurunan terma hidrogen. Komposit lapisan silika dengan jarak antara liang sebanyak 4.1 nm telah berjaya disintesis sebagai filem nipis, dengan hanya menggunakan trinuklear emas(I) pirazolat kompleks (**[Au3Pz3]C10TEG**) yang bersifat amfifilik sebagai templat. Berbeza jika dibandingkan dengan komposit dan kompleks **[Au3Pz3]C10TEG** yang telah melalui kaedah pengkalsinan pada suhu at 450ºC selama 3 jam, kaedah penurunan terma hidrogen pada suhu 250ºC selama 2 jam menghasilkan gambar mikroskop electron pancaran (TEM) dan corak pembelauan yang lebih kecil (14.5 nm) dan homogen dengan saiz zarah hampir 44% berada dalam lingkungan antara 10 hingga 20 nm. Pengurangan purata saiz zarah yang terhasil menggunakan strategi baru ini boleh dilihatkan berdasarkan peralihan ke hujung merah spektrum terhadap permukaan resonans plasmon (SPR) daripada 518 nm (**AuNPs** yang terhasil daripada **[Au3Pz3]C10TEG** komplek) dan 544 (hasil dari pengkalsinan) kepada 558 nm.

Kata kunci: Emas berzarah nano; nanokomposit lapisan silika; saiz zarah; penurunan terma hidrogen

1.0 INTRODUCTION

In chemistry and materials science, gold nanoparticles (**AuNPs**) have been widely used for many applications such as optics, electronics, energy membranes, catalysts, medicine, chromatography, drug delivery, photo-imaging, biological sensing, magnetic materials, and pigmentation [1, 2]. **AuNPs** with particle size less than 10 nm can provide enhancement of surface area thus give high activity especially in catalytic reaction. Moreover, the unique properties of **AuNPs** also depend on their particle and inter-particle sizes, nature of protecting organic shells and support as well as metal-support interface interactions [3].

Nowadays, **AuNPs** can be prepared using several methods such as calcination, thermal hydrogen reduction, and photo-reduction [4-6]. Recently, channels of mesoporous silica with size between 2 to 50 nm have been used as an inorganic hosts for growing and controlling the size of **AuNPs**, where two strategies have been employed for encapsulating the nanoparticles in the mesoporous silica. The first strategy is post-synthetic grafting method by involving mixing of metal sources with functionalized

mesoporous silica [7], while another one is the mixing of metal sources with the mixture of surfactants and silica sources via the co-condensation method [8]. However, agglomeration and non-homogeneous distribution as well as low loading of **AuNPs** in the channels of mesoporous silica are still the main problems of the above methods. On the other hand, in 2001, Aida *et al*. [9] and Brinker *et al*. [10] have independently reported that mesoporous silica nanocomposites consisting dense filling of organic functional groups in the silicate nanochannels can be prepared using diacetylenic monomer amphiphiles as functional templates in the sol-gel synthesis. Compared to statistical post-loading approaches, the sol-gel synthesis of mesoporous silica with functional template was more preferred due to its high possibility in dense filling of the organic functional groups into the silicate nanochannels. Therefore, in our work, we have reported a strategy based on amphiphilic functional surfactant of self-assembled metal complex via metallophilic interaction arranged one-dimensionally inside the channels of mesoporous silica, where the metal sources were attached to the surfactant molecules. In previous reports, by using trinuclear gold (I) pyrazolate complex bearing an amphiphilic side chains (**[Au3Pz3]C10TEG**) as a template in the sol-gel synthesis [11, 12], mesoporous silica film nanocomposite having a hexagonal geometry (**[Au3Pz3]C10TEG/silica$_{hex}$**) with high thermal resistivity [13] and perfect self-repairing properties [11, 14] was successfully fabricated. Moreover, this metal complex also was successfully used as both a template in the sol-gel synthesis [11-14] and as metal source in the formation of **AuNPs** by using calcination method [15], considering the gold sources was already inside the mesoporous silica channels. However, the resulting **AuNPs** gave a large particle size in the range between 20 to 30 nm (43%) and the rest with sizes more than 30 nm as being reported in our previous work. Hence, in this study we further demonstrate the synthesis of **AuNPs** in the channels of mesoporous silica by using thermal hydrogen reduction that capable to give particle size less than twice compared to the reported calcination method.

■2.0 EXPERIMENTAL

2.1 General

Proton (^{1}H-) and carbon (^{13}C-) nuclear magnetic resonance (NMR) spectra were recorded on a Bruker AVANCE 300 MHz NMR spectroscopy, where chemical shifts were determined with respect to deuterated chloroform ($CDCl_3$) at chemical shift δ of 7.24 ppm for ^{1}H-NMR and δ 77.0 ppm for ^{13}C-NMR spectroscopy as internal standards. XRD measurements were carried out at room temperature on a Bruker D8 Advance diffractometer, with Cu$K\alpha$ radiation (40 kV, 40 mA) and a step size of 0.02° at a scan speed of 2° min^{-1} from 2θ = 1.5 to 60°. Ultraviolet-visible (UV-vis) spectra were recorded on a Thermo Scientific model GENESYS 10S UV–vis spectroscopy at a scan speed 100 nm min^{-1}. TEM images were obtained by using a JEOL JEM-2100 operating at 200 kV. Mass spectra were recorded on a AB Sciex MALDI- TOF/TOF™ 5800 Spectrometry system with ion positive ionization and reflection mode. Dithranol (1,8,9-antracenetriol) was used as a matrix in chloroform. Fourier Transform Infrared (FT-IR) spectra were recorded on a Nicolet iS50 FT-IR Spectrometer Thermo Scientific, where the sample preparation was done by using potassium bromide (KBr) pellet. Reactions were monitored by thin-layer chromatography carried out on 0.2 mm Merck pre-coated silica gel plates. Calcination of the silica films was carried out in air at 450°C for 3 h using Nabertherm model electronic muffle furnace, while the thermal hydrogen reduction was carried out in hydrogen environment at 250°C for 2 h using Carbolite model quartz tube furnace.

2.2 Synthesis of [Au3Pz3]C10TEG

[Au3Pz3]C10TEG was prepared as according to synthetic protocols reported previously by Lintang *et al*. [11, 12]. Typically, to **C10TEGPzH** (400.0 mg, 0.35 mmol) was added [Au(SMe_2)]Cl (103.2 mg, 0.35 mmol) in dry tetrahydrofuran (THF; 20.00 mL) and stirred for 5 min at room temperature. To this mixture, potassium hydroxide (KOH; 0.26 M, 200.0 mg) in dry methanol (MeOH; 1.40 mL) was added using Schlenk technique and stirred for 12 h under inert condition at room temperature. The mixture was *in-situ* purified *via* filtration from insoluble substances, and the filtrate was evaporated. The residue was subjected to column chromatography using silica gel with mixture of ethyl acetate and methanol (AcOEt/MeOH in ratio of 10:1) as an eluent. Each fraction was collected and evaporated to dryness under reduced pressure and freeze–dried from benzene, to give **[Au3Pz3]C10TEG** as a pale–yellow sticky solid with 69% yield (300.0 mg, 0.08 mmol).

The structure elucidation for **C10TEGPzH** are as follows; NMR δ_H (300 MHz, $CDCl_3$, 25 °C) ppm with label of proton as shown in Figure 1: 6.25 (s, 1.72 H, **h** = ArH), 3.92-3.84 (overlapped, 5.19 H, **g** = OCH_2, **i** = $ArCH_2$), 3.67-3.51 (overlapped, 36.00 H, **b** = CH_2CH_2O $CH_2CH_2OCH_2CH_2$), 3.47-3.36 (overlapped, 15.00 H, **c** = OCH_2, **a** = OCH_3), 2.15 (s, 5.07 H, **j** = CH_3), 1.75-1.61 (overlapped, **f** = CH_2, **d** = CH_2), 1.41-1.20 (overlapped, 43.66 H, **e** = $(CH_2)_6$); NMR δ_C (75 MHz, $CDCl_3$, 25 °C) ppm with label of carbon as shown in Figure 2: 152.53 (**l** = Ar), 141.94 (**q** = pyrazole (py)-CH_3), 135.68 (**k** = ArO), 128.35-128.09 (**n** = Ar), 113.33 (**p** = py-C), 106.45 (**m** = Ar), 72.88 (**j** = OCH_2), 72.50 (**b** = OCH_2), 70.15 (**e** = OCH_2), 70.03 (**d** = CH_2CH_2O), 69.62 (**c** = CH_2O), 68.66 (**j** = OCH_2), 58.48 (**a** = CH_3O), 29.88 (**f** = OCH_2CH_2), 29.63 (**o** = $ArCH_2$), 25.65 (**g** = $CH_2CH_2CH_2CH_2CH_2$, 29.21 (**h** = $ArOCH_2CH_2CH_2$) and 10.41 (**r** = CH_3); IR ν_{max} (KBr) cm^{-1}: 3381 (N-H), 2918 (C-H), 2393 (N-H), 1623 (C=C), 1464 (C=N), 1368, 1106, 1073, 819, 607 (C-H aromatic out of plane); MALDI-TOF-MS (dithranol as a matrix, m/z); [M+H$^+$] calculated for **$C_{63}H_{116}N_2O_{15}$** (**C10TEGPzH**): 1141.84; found 1141.83.

The structure elucidation for **[Au3Pz3]C10TEG** are as follows; NMR δ_H (300 MHz, $CDCl_3$, 25 °C) ppm with label of proton as shown in Figure 1: 6.25 (s, 6 H, **h** = ArH), 3.89-3.85 (overlapped, 18.00 H, **g** = OCH_2, **i** = $ArCH_2$), 3.63-3.50 (overlapped, 122.00 H, **b** = $CH_2CH_2OCH_2CH_2OCH_2CH_2$), 3.43-3.39 (overlapped, **c** = OCH_2), 3.35 (s, 27.00 H, **a** = OCH_3), 2.15 (s, 15.00 H, **j** = CH_3), 1.75–1.54 (overlapped, 428.00 H, **f** = CH_2, **d** = CH_2), 1.26-1.20 (overlapped, 146.00 H, **e** = $(CH_2)_6$); NMR δ_C (75 MHz, $CDCl_3$, 25 °C) ppm with label of carbon as shown in Figure 2: 153.00 (**l** = Ar), 146.60 (**q** = pyrazole (py)-CH_3), 136.56 (**k** = ArO), 135.95 (**n** = Ar), 113.90 (**p** = py-C), 106.82 (**m** = Ar), 73.36 (**j** = OCH_2), 71.92 (**b** = OCH_2), 70.50 (**e** = OCH_2), 70.60-70.48 (**d** = CH_2CH_2O), 70.20 (**c** = CH_2O), 69.17 (**j** = OCH_2), 58.97 (**a** = CH_3O), 30.32-30.11 (**f** = OCH_2CH_2), 29.64-29.46 (**g** = $CH_2CH_2CH_2CH_2CH_2$), 26.10 (**h** = $rOCH_2CH_2CH_2$), and 12.29 ppm (**r** = py-CH_3); IR ν_{max} (KBr) cm^{-1}: 3484 (O-H), 2939 (C-H), 1645 (C=C), 1477 (C=N), 1370, 1141, 1014, 712 (C-H aromatic out of plane); MALDI-TOF-MS (dithranol as a matrix, m/z): [M+Na$^+$] calculated for **$C_{189}H_{345}N_6Au_3O_{45}Na$** (**[Au3Pz3]C10TEG**): 4033.38; found 4033.39.

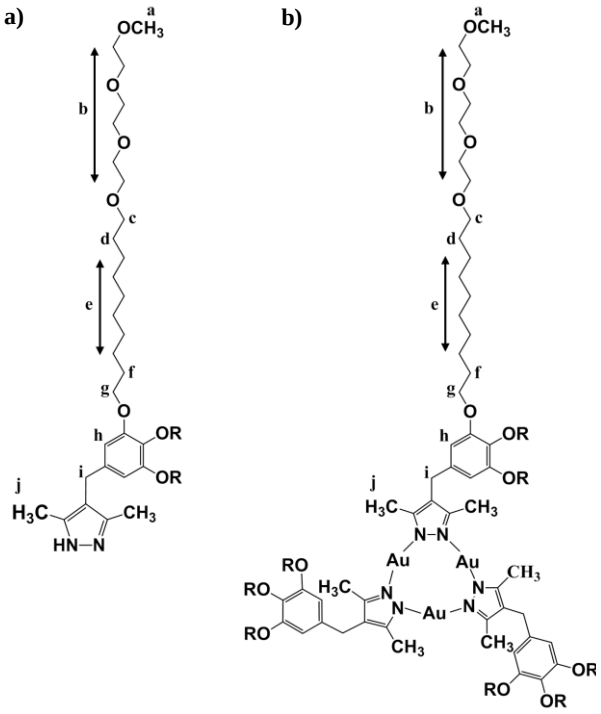

Figure 1 Representative structure of a) **C10TEGPzH** and b) **[Au3Pz3]C10TEG** for ^{1}H-NMR spectra

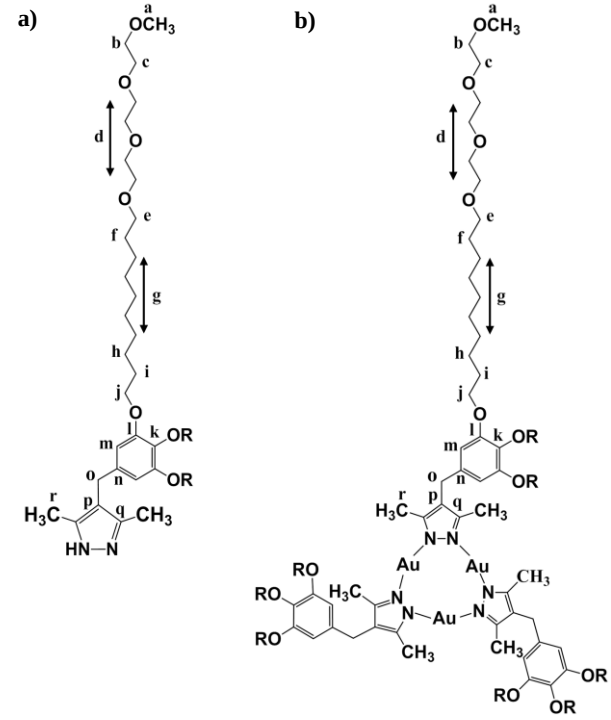

Figure 2 Representative structure of a) **C10TEGPzH** and b) **[Au3Pz3]C10TEG** for ^{13}C-NMR spectra

2.3 Sol-gel Synthesis of [Au3Pz3]C10TEG/silica$_{hex}$

The sol-gel synthesis was also done as according to synthetic protocols reported previously by Lintang *et al*. [11, 12]. For the sol-gel synthesis of mesostructured silica/gold nanocomposites (**[Au3Pz3]C10TEG/silica$_{hex}$**), an acidic aqueous ethanol solution in water (EtOH, 61.6 mg, 1.25 mmol; HCl, 0.3 mg, 2.99 x 10^{-3} mmol; H_2O, 11.9 mg, 0.70 mmol) with a mixture of **[Au3Pz3]C10TEG** (10.0 mg, 2.49 x 10^{-3} mmol) and tetrabutyl orthosilicate (TBOS, 48.0 mg, 1.49 x 10^{-1} mmol) was held for 12 h at room temperature as colloidal solution. The ratio used during this process was ([**[Au3Pz3]C10TEG**]/ [TBOS]/ [EtOH]/ [HCl]/ [H_2O] = 1:60:504:1.2:266) upon partial oligomerization of TBOS took place. The resulting viscous solution was spin-coated on a quartz plate at 3000 rpm for 15 s, affording a transparent film which dried in air for 24 h at room temperature. For the formation of **AuNPs**, thermal hydrogen reduction was carried out by flowing hydrogen gas to the quartz tube furnace containing silica films with flow rate of 30 mL min^{-1}, at 250°C for 2 h. The research design was summarized as shown in Scheme 1;

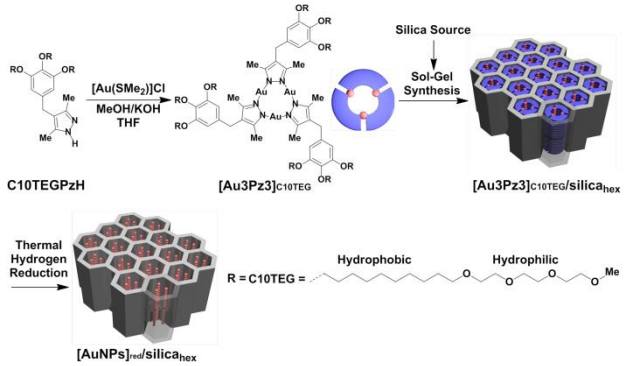

Scheme 1 Schematic representation for the synthesis of gold(I) pyrazolate complex (**[Au3Pz3]C10TEG**) from pyrazole ligand (**C10TEGPzH**) and followed by the sol-gel synthesis to form mesostructured silica/gold nanocomposites (**[Au3Pz3]C10TEG/silica$_{hex}$**) before reduced to form **[AuNPs]/silica$_{hex}$**

3.0 RESULTS AND DISCUSSION

3.1 Structural Analysis of Mesoporous Silica Composite

Small-angle area of XRD patterns can be used to study the formation of mesoporous silica [6]. In Figure 3A, diffraction peaks at 2θ = 2.16° (d_{100}), 3.70° (d_{110}), and 4.30° (d_{200}) indicate the characteristics of a hexagonal mesoporous silica [11, 12]. The calculation of the interpore distance at 2θ = 2.16° by using Bragg's law was found to be 4.1 nm. New diffraction peaks at 2θ = 2.90° ($d_{100,}$ after calcination) and 2θ = 2.34° ($d_{100,}$ after thermal hydrogen reduction) were observed to indicate preservation of hexagonal structure of the silica (Figure 3B and 3C) having an interpore distance of 3.0 and 3.5 nm, respectively. Interestingly, after thermal hydrogen reduction, not only an intense d_{100} peak was shown to indicate high quality of mesoporous silica, but also the size of mesoporous silica channels was increased compared to calcination method, thus suggesting under thermal hydrogen reduction the hexagonal channels of mesoporous silica do not disrupted drastically and shrinkage of TEG interpenetration in the silica wall is slowly occured. From the TEM images in Figure 4, structure of mesoporous silica having uniform hexagonal arrangement was clearly observed, thus supporting the XRD data of the as-fabricated silica film of the gold nanocomposites (**[Au3Pz3]C10TEG/silica$_{hex}$**) having interpore distance of 4.0 to 5.0 nm.

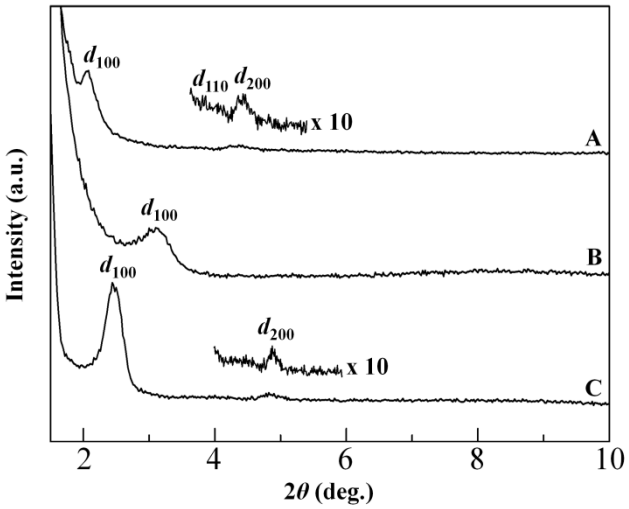

Figure 3 XRD patterns of **[Au3Pz3]C10TEG/silica$_{hex}$** of A) before calcination, B) after calcination at 450ºC for 3 h to form **[AuNPs]$_{cal}$/silica$_{hex}$**, and C) after reduction at 250ºC for 2 h to form **[AuNPs]$_{red}$/silica$_{hex}$**

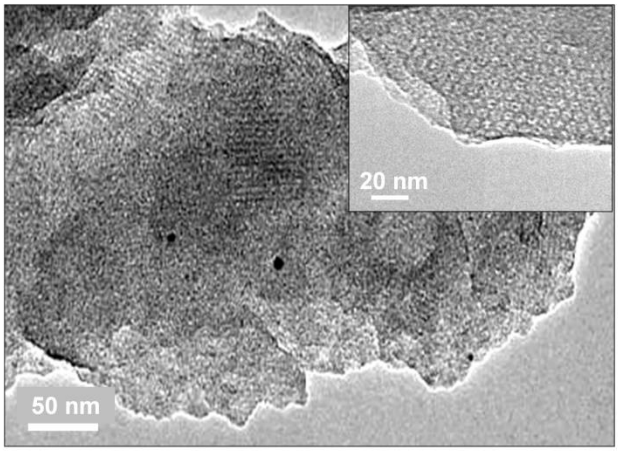

Figure 4 TEM image of **[Au3Pz3]C10TEG/silica$_{hex}$** with the inset figure having scale bar of 20 nm

3.2 Particle Size Analysis of AuNPs

The XRD patterns at wide angle area were used to confirm the formation of **AuNPs** [1]. In Figure 5, diffraction peaks at 2θ = 38.20º were observed for all samples due to presence of **AuNPs** with d_{111} having a cubic phase [5]. Scherrer's equation for the determination of particle size of **[AuNPs]$_{red}$/silica$_{hex}$** was 14.5 nm in diameter (Figure 5C). Interestingly, this size was quite less than that of **AuNPs** formed from the bulk (41.4 nm, Figure 5A) and calcined (27.8 nm, Figure 5B). These results also indicate the formation of **AuNPs** at lower temperature under hydrogen environment, where it can give more controllable size for growing of **AuNPs** in the channels of mesoporous silica.

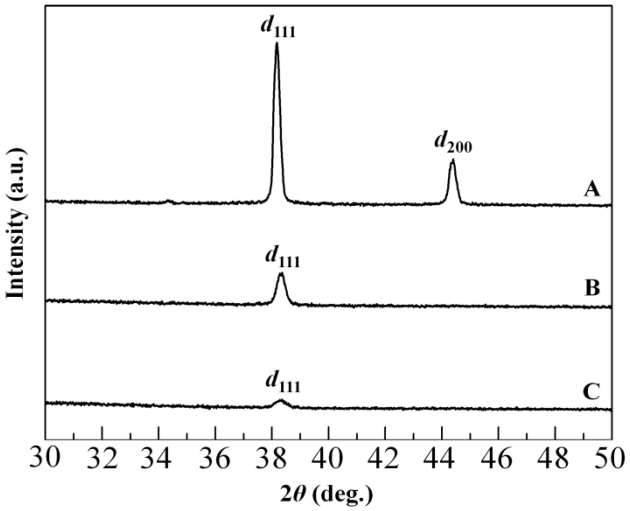

Figure 5 XRD patterns of A) bulk **[Au3Pz3]C10TEG** after calcination to form **AuNPs**, B) **[AuNPs]$_{cal}$/silica$_{hex}$**, and C) **[AuNPs]$_{red}$/silica$_{hex}$**

TEM measurement was used to study the formation of **AuNPs** [5]. Generally, as being reported in our previous work [15], calcination resulted **AuNPs** with most of the particle size in the range of 20 to 30 nm (43%), while the rest having particle size more than 30 nm as shown in Figure 6a(B). In contrast to the calcination, thermal hydrogen reduction was proved to produce smaller and homogeneous distribution of **AuNPs** with most of particle size between 10 to 20 nm (44%), less than 10 nm (16%), as well as other sizes between 20 to 30 nm (27%), 30 to 40 nm (8%), 40 to 50 nm (2%), and 50 to 60 nm (3%) as shown in Figure 6b(B). The TEM result after thermal hydrogen reduction was also in good agreement with calculation using Scherrer's equation of the XRD data.

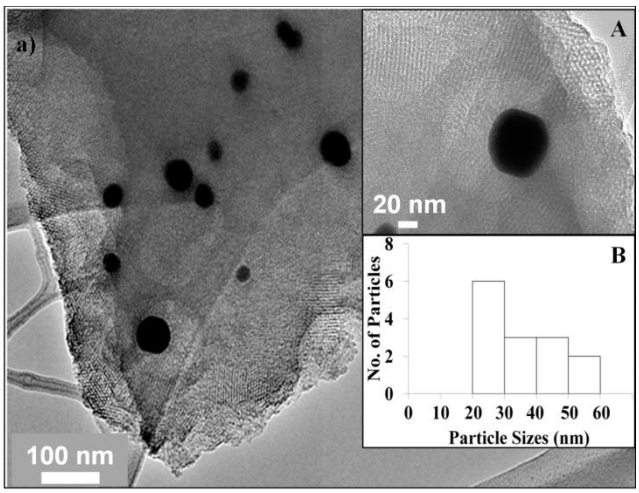

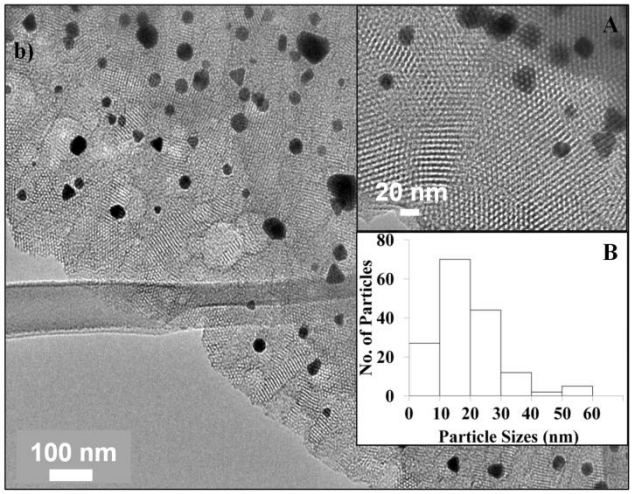

Figure 6 TEM images of a) **[AuNPs]$_{cal}$/silica$_{hex}$** and b) **[AuNPs]$_{red}$/silica$_{hex}$** with the A) inset figure having scale bar of 20 nm, and B) histogram of particle size distribution

3.3 Optical Properties of AuNPs

UV-vis spectroscopy can be used to identify the appearance of SPR properties for **AuNPs** [5]. Before the calcination or themal hydrogen reduction was conducted, the bulk **[Au3Pz3]C10TEG** was in a form of yellow sticky solid while the **[Au3Pz3]C10TEG/silica$_{hex}$** as colourless thin film after spin-coated on glass substrate as shown in the Figure 7a and b. After the treatment, the colourless thin film was changed to light-pink for calcination (Figure 7c) and purplish-pink for thermal hydrogen reduction (Figure 7d) due to the presence of the **AuNPs**.

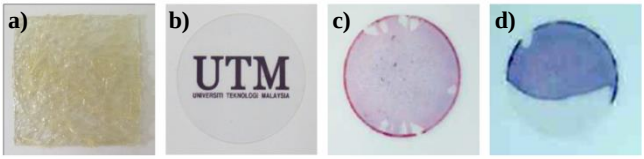

Figure 7 The thin films of a) bulk **[Au3Pz3]C10TEG** on glass substrate**,** b) **[Au3Pz3]C10TEG/silica$_{hex}$** as colourless thin film, c) light-pink colour thin film was formed after calcination at 450°C for 3 h, and d) purplish-pink thin fim was formed after thermal hydrogen reduction at 250°C for 2 h

In Figure 8, new peak at 558 nm after thermal hydrogen reduction was observed to indicate the SPR properties of the **AuNPs**, as there are noSPR bands of the bulk gold(I) pyrazolate complex and as-synthesized silica film as shown in inset figure. Moreover, the absorption bands with the peaks less than 350 nm for both **[Au3Pz3]C10TEG** and **[Au3Pz3]C10TEG/silica$_{hex}$** are due to π–π stacking of benzene rings [11, 12]. Interestingly, the absorption peak of **[Au3Pz3]C10TEG/silica$_{hex}$** was sharper and narrower than that of the bulk, proposing the phenomenon of dense filling of the complex as columnar assembly in the channels of mesoporous silica. In addition, the SPR band of the **AuNPs** formed in the channels of mesoporous silica was red-shifted from 518 (bulk **AuNPs**) and 544 nm (**[AuNPs]$_{cal}$/silica$_{hex}$**) to 558 mm (**[AuNPs]$_{red}$/silica$_{hex}$**) which can be explained by the decrease of the average particle size as reported by Fukuoka *et al*. [5].

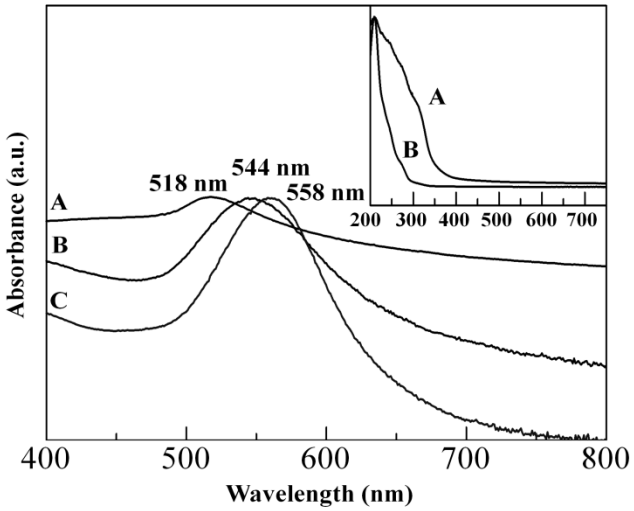

Figure 8 UV-vis spectra of the resulting **AuNPs** with A) bulk **AuNPs**, B) **[AuNPs]$_{cal}$/silica$_{hex}$**, and C) **[AuNPs]$_{red}$/silica$_{hex}$**. The inset figure is the UV-vis spectra before the formation of **AuNPs** with A) bulk **[Au3Pz$_3$]C10TEG** and B) **[Au3Pz3]C10TEG/silica$_{hex}$**

■4.0 CONCLUSION

It was demonstrated that thermal hydrogen reduction of mesoporous silica composite containing dense filling of gold precursors in the silicate nanochannels gave smaller size of **AuNPs (**14.5 nm) from the diffraction peak at 2θ = 38.20^o, microscope images, and SPR band compared to the calcination of the as-synthesized mesoporous silica (27.8 nm) and bulk **[Au3Pz3]C10TEG** (41.4 nm). Moreover, it was found that this method also showed formation of more homogenous distribution of the particle. Future researches will challenge on the controlled-size synthesis of the **AuNPs** as according to the size of the silicate nanochannels by controlling the heating rate and temperature during the thermal hydrogen reduction.

Acknowledgement

The authors thank Universiti Teknologi Malaysia (UTM), Malaysia for characterization facilities. The authors also thank Ministry of Higher Education (MOHE) through Research University Grant Scheme (RUGS Tier 1 2013, Vote No. Q.J130000.2526.04H02) and Ministry of Science, Technology, and Innovation (MOSTI) through Flagship Research Grant for NanoMalaysia COE 2011 (Vote No. R.J130000.7762.4S017), Malaysia for the financial supports. Mohamad Azani Jalani also acknowledges the financial support from UTM through Zamalah Postgraduate Scholarship (UTM.J.10.01/13.14/1/127/1(900308086095)).

References

[1] Cao, Y., J. Huang, L. C. Wang, Y. M. Liu, H. Y. He, and K. N. Fan. 2011. Gold Nanoparticles Supported on Hydroxylapatite as High Performance Catalysts for Low Temperature CO Oxidation. *Applied Catalysis B: Environmental*. 101(3–4): 560–569.

[2] Niidome, T., D. Pissuwan, and M. B. Cortie. 2011. The Forthcoming Applications of Gold Nanoparticles in Drug and Gene Delivery Systems. *Journal of Controlled Release*. 149(1): 65–71.

[3] Astruc, D. and M. C. Daniel. 2004. Gold Nanoparticles: Assembly, Supramolecular Chemistry, Quantum-Size-Related Properties, and

Applications toward Biology, Catalysis, and Nanotechnology. *Chemical Review*. 104(1): 293–346.

[4] Wu, Y., C. Niu, Z. Wang, Z. Li, and R. Li. 2009. Synthesis and Shapes of Gold Nanoparticles by using Transition Metal Monosubstituted Heteropolyanions as Photocatalysts and Stabilizers. *Frontiers of Chemistry in China*. 4(1): 44–47.

[5[Fukuoka, A., H. Araki, Y. Sakamoto, N. Sugimoto, J. Kimura, T. Higuchi, S. Inagaki, and M. Ichikawa. 2004. Template Synthesis of Nanoparticles Arrays of Gold, Platinum, and Palladium in Mesoporous Silica Films and Powders. *Journal of Materials Chemistry*. 14(4): 752–756.

[6] Fukuoka, A., H. Araki, Y. Sakamoto, N. Sugimoto, H. Tsukada, Y. Kumai, Y. Akimoto, and M. Ichikawa. 2002. Template Synthesis of Nanoparticle Arrays of Gold and Platinum in Mesoporous Silica Films. *Nano Letters*. 2(7): 793–795.

[7] Kumar, R., A. Ghosh, C. R. Patra, P. Mukherjee, and M. Sastry. 2003. Preparation and Stabilization of Gold Nanoparticles Formed by In Situ Reduction of Aqueous Chloroaurate Ions Within Surface-Modified Mesoporous Silica. *Microporous and Mesoporous Materials*. 58(3): 201–211.

[8] Somorjai, G. A., Z. Konya, V. F. Puntes, I. Kiricsi, J. Zhu, J. W. Ager, M. K. Ko, H. Frei, and P. Alivisatos. 2003. Synthetic Insertion of Gold Nanoparticles into Mesoporous Silica. *Chemistry of Materials*. 15(6): 1242–1248.

[9] Aida, T. and K. Tajima. 2001. Photoluminescent Silicate Microsticks Containing Aligned Nanodomains of Conjugated Polymers by Sol-Gel Based In Situ Polymerization. *Angewandte Chemie International Edition.* 40(20): 3803–3806.

[10] Brinker, C. J., Y. Lu, Y. Yang, A. Sellinger, M. Lu, J. Huang, H. Fan, R. Haddad, G. Lopez, A. R. Burns, D. Y. Sasaki, and J. Shellnut. 2001. Self-Assembly of Mesoscopically Ordered Chromatic Polydiacetylene/Silica Nanocomposites. *Nature*. 410(6831): 913–917.

[11] Lintang, H. O., K. Kinbara, Tanaka, T. Yamashita, and T. Aida. 2010. Self-Repair of a One-Dimensional Molecular Assembly in Mesoporous Silica by a Nanoscopic Template Effect. *Angewandte Chemie International Edition*. 49(25): 4241–4245.

[12] Lintang, H. O., K. Kinbara, K. Tanaka, T. Yamashita, and T. Aida. 2012. Metal-Ion Permeation in Congested Nanochannels: The Exposure Effect of Ag^+ Ions on the Phosphorescent Properties of a Gold(I)–Pyrazolate Complex that is Confined in the Nanoscopic Channels of Mesoporous Silica. *Chemistry-An Asian Journal*. 7(9): 2068–2072.

[13] Lintang, H. O., K. Kinbara, and T. Aida. 2012. Thermally Resistive Phosphorescent Molecular Assembly in the Channels of Mesoporous Silica Nanocomposites. *Proceedings of International Conferences on Enabling Science and Nanotechnology (ESciNano)*. Article Number 6149684. ISBN: 978-1-4577-0799-5.

[14] Lintang, H. O., K. Kinbara, T. Yamashita, and T. Aida. 2010. Heating Effect of a One-Dimensional Molecular Assembly on Self-Repairing Capability in the Nanoscopic Channels of Mesoporous Silica. *Proceedings of International Conferences on Enabling Science and Nanotechnology (ESciNano)*. Article Number 5700970. ISBN: 978-1-4244-8853-7.

[15] Jalani, M. A., L. Yuliati, S. Endud, and H. O. Lintang. 2014. Synthesis of Mesoporous Silica Nanocomposites for Preparation of Gold Nanoparticles. *Advanced Materials Research.* 925: 233–237.

[16] Raptis, R. G. and G. Yang. 2003. Supramolecular Assembly of Trimeric Gold(I) Pyrazolates through Aurophilic Attractions. *Inorganic Chemistry*. 42(2): 261–263.